



Received: 2014.10.02
Accepted: 2014.11.04
Published: 2015.02.11

Authors' Contribution:

- A** Study Design
- B** Data Collection
- C** Statistical Analysis
- D** Data Interpretation
- E** Manuscript Preparation
- F** Literature Search
- G** Funds Collection

Brain Magnetic Resonance Imaging and Magnetic Resonance Spectroscopy Findings of Children with Kernicterus

Sahabettin Sari¹□, Alpaslan Yavuz²□, Abdussamet Batur²□, Aydın Bora²□, Huseyin Caksen²□

¹ Department of Pediatrics, Baskale State Hospital, Van Sehiri, Turkey

² Department of Radiology, Yuzuncuyil University Dursun Odabas Medical Center, Van, Turkey

Author's address: Abdussamet Batur, Department of Radiology, Yuzuncuyil University Dursun Odabas Medical Center, Van, Turkey, e-mail: drsamet56@yahoo.com

Background:

The term kernicterus, or bilirubin encephalopathy, is used to describe pathological bilirubin staining of the basal ganglia, brain stem, and cerebellum, and is associated with hyperbilirubinemia. Kernicterus generally occurs in untreated hyperbilirubinemia or cases where treatment is delayed. Magnetic resonance imaging (MRI)-based studies have shown characteristic findings in kernicterus. The objective of our study was to describe the role of ¹H magnetic resonance spectroscopy (MRS) in demonstrating these metabolic changes and to review conventional MRI findings of kernicterus.

Material/Methods:

Forty-eight pediatric cases with kernicterus were included in this study. MRI and MRS examinations were performed on variable dates (10–29 days after birth). NAA, Cr, Cho, NAA/Cr, NAA/Cho, and Cho/Cr values were evaluated visually and by computer analysis.

Results:

There was no statistically significant difference between the NAA and Cho levels in the acute kernicterus patients and the control group (healthy patients), whereas both were significantly elevated in the chronic kernicterus patients. Both the mean NAA/Cr and Cho/Cr ratio values were significantly higher in the acute and chronic cases compared to the control group. The NAA/Cho ratio value was statistically lower in the acute cases than in the control group while it was similar in the chronic cases.

Conclusions:

Conventional MR imaging and ¹H-MRS are important complementary tools in the diagnostics of neonatal bilirubin encephalopathy. This study provided important information for applying these MR modalities in the evaluation of neonates with bilirubin encephalopathy.

MeSH Keywords:

Infant, Newborn • Kernicterus • Magnetic Resonance Spectroscopy

PDF file:

<http://www.polradiol.com/abstract/index/idArt/892643>

Background

The term kernicterus, or bilirubin encephalopathy, is used to describe pathological bilirubin staining of the basal ganglia, brain stem, and cerebellum, and is associated with hyperbilirubinemia. The non-conjugated bilirubin reaches the brain and acts as a neurotoxin, often in association with conditions that impair the blood–brain barrier (e.g. sepsis). This condition occurs primarily in neonates (infants and newborns) and may rarely occur in adults [1]. Neonatal

jaundice is easily treatable with phototherapy, albumin infusion, or exchange transfusion [2,3]. However, the damage inflicted on the brain by bilirubin is not always reversible and can result in cerebral palsy, deafness or hearing loss, impairment of upward gaze, and enamel dysplasia of the primary teeth [4]. Magnetic resonance imaging (MRI)-based studies have shown characteristic findings of kernicterus: signal intensity increase on T2-weighted images (WI) of the globus pallidus (GP), subthalamic nuclei, and hippocampus in the subacute and chronic phases of

kernicterus [5,6]. Increased signal intensity on T1WI in the globus pallidus and subthalamic nuclei in the acute phase have previously been reported in the literature [7]. High bilirubin levels cause the inhibition of glutamate (Glu) uptake by astrocytes [8], and increased extracellular glutamate concentrations cause neuronal death due to hyperexcitation of the postsynaptic neurotransmitter receptors [9]. The objective of our study was to describe the role of ^1H magnetic resonance spectroscopy (MRS) in demonstrating these metabolic changes and to review conventional MRI findings of kernicterus in the light of previously published studies.

Material and Methods

Fifty pediatric cases with kernicterus referred to the Yuzuncu Yil University Pediatric Neurology Department were included in this study. All the patients' parents were asked for their written consent, and ethical authorization from the university ethics committee was obtained. Two infants were excluded from the study due to the co-existence of additional disorders (urinary infection, respiratory distress, major congenital malformations, congenital heart disease, sepsis, or acidosis) that could predispose to bilirubin neurotoxicity. The remaining 48 patients were divided into two groups: Group 1 consisted of nine acute patients [four males (45.5%) and five females (55.5%)], and Group 2 comprised 39 chronic hyperbilirubinemia cases [29 males (74.4%) and 10 females (25.6%)]. Infants with a history of neonatal asphyxia or clinic and radiologic hypoxic ischemic encephalopathy findings were excluded from the study.

Patients with an initial diagnosis of kernicterus with typical clinical findings (jaundice, encephalopathy, lethargy, hypotonia, and lack of nursing) and high serum bilirubin levels [total serum bilirubin (TSB) >25 mg/dL] were included in Group 1 prospectively. Group 1 cases were divided into two groups depending on the gestational week, i.e., Group 1a: preterm (four cases, 35–36 weeks); Group 1b: term (five cases, 38–40 weeks). Each patient's age, sex, gestational week, birth weight, total serum bilirubin level, and therapy modality was recorded. The infant and maternal blood type mismatches, Rh-ABO, were marked. Neurological examinations were performed at initial admission and four months later. MRI and MRS examinations were performed on variable dates (10–29 days after birth).

Group 2 was constituted by a retrospective review from June 2006 to June 2009 and was observed between June 2009 and January 2011. The achievable medical data (initial physical, laboratory, and radiological examination records) were gathered from archives. Previous achievable MRI examinations of Group 2 cases were also reviewed. Instant control MRI and MRS findings were noted.

A 1.5 Tesla (T) MR imaging system (Siemens Magnetom Symphony, Erlangen, Germany) was used for all the patients. MRI examinations were conducted under sedation (50 mg/kg chloral hydrate, maximum 1 g per os). The following MRI sequences were acquired: axial, sagittal T1WI spin echo (repetition time [TR]: 490 ms; echo time [TE]: 9.4 ms); axial, sagittal T2WI turbo spin echo (TR: 3500 ms;

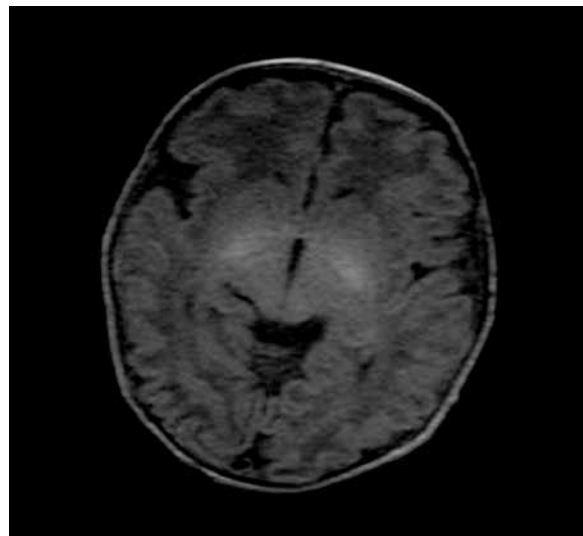


Figure 1. A 23-day-old female, T1-weighted MRI demonstrated an increased intensity in the bilateral globus pallidus and mesencephalon.

TE: 90 ms); and axial fluid attenuation inversion recovery (FLAIR) (TR: 7850 ms; TE: 108 ms; inversion time [TI]: 2600 ms). Group 1 patients with high T1W signal intensities in GP (all nine Group 1 cases) and Group 2 patients with abnormal T2W signal intensity changes in GP (24 of 39 cases) were examined with MRS. After defining the size and location of the lesions in routine T1WI and T2WI MRI sequences, short and long TR/TE 1500/30–135 single voxel brain ^1H -MRS was performed. The voxel sizes were at least $1 \times 1 \times 1$ cm and maximally $2 \times 2 \times 2$ cm. Normal and affected brain tissues were examined. The NAA, Cr, Cho, NAA/Cr, NAA/Cho, and Cho/Cr values were evaluated visually and by computer analysis. The brain MRS values were commented on in the light of the healthy control group scale reported by Kreis et al. [10].

Statistical analysis: The mean, standard deviation, and minimum and maximum values were referred to as continuous variables, and the categorical variables were expressed as numbers and percentages. The Mann-Whitney U test was used in the comparison of continuous variables. Moreover, the one-sample t-test was used in the comparison of Group 1a and 1b with the control group. The statistical analysis was performed with SPSS software (version 13.0). The probability level of less than 0.05 was considered significant.

Results

Neurological physical examinations were carried out at the initial admission of Group 1 cases, and the findings were as follows: hypotonia, lack of nursing, and lethargy. In Group 1, the mean age was 5.22 ± 1.7 days (2–8 days), and the mean gestational age was 37.89 ± 2.1 weeks (35–40 weeks). The mean weight and mean birth weight of Group 1 patients were 2615 ± 451.3 g (2000–3280 g) and 2791 ± 407.99 g (2300–3300 g), respectively. The mean TSB was 31.1 ± 4.9 mg/dL (26–40 mg/dL). Two cases (22.2%) with Rh mismatch and three cases with ABO mismatch (33.3%) were determined in Group 1. High bilirubin levels with

Table 1. Group 1 initial and control MRI findings.

Patient/ sex	Initial MRI			Control MRI		
	T1WI	T2WI	FLAIR	T1WI	T2WI	FLAIR
1/F	Increased signal intensity in bilateral GPi and mesencephalone	Normal	Normal	Normal	Normal	Normal
2/F	Increased signal intensity in bilateral GPe and GPi	Increased signal intensity in hippocampus, minimally decreased signal intensity due to white matter myelination delay	Increased signal intensity in the hippocampus	Mild lateral ventricular dilatation and minimal diffuse callosal thinning	Mild lateral ventricular dilatation and minimal diffuse callosal thinning	Mild lateral ventricular dilatation and minimal diffuse callosal thinning
3/M	Increased signal intensity in bilateral GPi	Minimal callosal thinning	Normal	Normal	Minimally increased signal intensity in GPi and GPe	Normal
4/M	Increased signal intensity in bilateral GPi and mesencephalone	Normal	Normal	Normal	Bilateral increased signal intensities in the white matter adjacent to the occipital and frontal horns of the lateral ventricle	Bilateral increased signal intensities in the white matter adjacent to the occipital and frontal horns of the lateral ventricles
5/F	Increased signal intensity in bilateral GPi, GPe, mesencephalone, caudate nucleus and lentiform nucleus.	Normal	Normal			
6/M	Increased signal intensity in bilateral GPi and mesencephalone	Normal	Normal	Normal	Normal	Normal
7/F	Increased signal intensity in bilateral GPe and GPi, Minimally decreased signal intensity in the white matter due to cerebral prematurity	Minimally increased signal intensity in the white matter due to cerebral prematurity	Minimally increased signal intensity in the white matter due to cerebral prematurity	Normal	Normal	Normal
8/F	Increased signal intensity in bilateral GPe and GPi, Minimally decreased signal intensity in the white matter due to cerebral prematurity	Minimally increased signal intensity in the white matter due to cerebral prematurity	Minimally increased signal intensity in the white matter due to cerebral prematurity	Normal	Normal	Normal
9/M	Increased signal intensity in bilateral GPe and GPi, Minimally decreased signal intensity in the white matter due to cerebral prematurity	Minimally increased signal intensity in the white matter due to cerebral prematurity	Minimally increased signal intensity in the white matter due to cerebral prematurity			

Table 2. Group 1a (preterm infants) MRS values.

Patient/sex/age (day)	TE (msec)	NAA (mmol/kg)	Cho (mmol/kg)	Cr (mmol/kg)	NAA/Cr	NAA/Cho	Cho/Cr
1/F/26	135	3.63	5.41	3.40	1.06	0.67	1.59
2/F/26	135	2.77	4.64	3.39	0.81	0.58	1.36
3/F/18	135	2.00	2.64	1.92	1.41	0.75	1.37
4/M/25	135	1.39	2.21	1.20	1.15	0.62	1.84

Normal values for preterm infants (Mean \pm standard deviation): NAA – 2.5 ± 0.6 mmol/kg; Cho – 2.1 ± 0.5 mmol/kg; Cr – 4.5 ± 0.4 mmol/kg; NAA/Cho – 1.99; NAA/Cr – 0.56; Cho/Cr – 0.47; [11].

Table 3. Group 1a (preterm infants) MRS values compared with the healthy control group.

Metabolites	Group 1a				Control group		
	Mean	St. deviation	Min.	Max.	Mean	St. deviation	P
NAA	2.45	0.97	1.39	3.63	2.50	0.60	0.921
Cho	3.73	1.54	2.21	5.41	2.10	0.40	0.147
Cr	2.48	1.10	1.20	3.40	4.50	0.40	0.050
NAA/Cho	0.66	0.07	0.60	0.76	1.19	0.00	0.050
NAA/Cr	1.02	0.14	0.82	1.16	0.56	0.00	0.013
Cho/Cr	1.54	0.22	1.37	1.84	0.47	0.00	0.001

Min. – minimum; Max. – maximum; St. deviation – standard deviation.

unexplained etiology (idiopathic) were revealed in four cases (44.4%).

In all Group 1 cases, bilateral, symmetrical, abnormally increased signal intensities in the globus pallidus were determined by T1WI (Figure 1). Premature signal intensity changes were revealed in three cases, but no additional abnormal changes were obtained in T2WI or FLAIR sequences. After therapy, control MRI examinations were performed in seven cases; four cases had normal MRI findings. Mild lateral ventricular dilatation and minimal diffuse callosal thinning was determined in one case. Minimally increased signal intensity in the globus pallidus externa and interna was detected by T2WI in one case; the T1WI and FLAIR sequences were normal. T2WI and FLAIR showed increased signal intensities in the white matter adjacent to the occipital and frontal horns of the lateral ventricle in one case. The initial and control MRI findings of Group 1 cases are summarized in Table 1.

The MRS findings of preterm newborns from Group 1a were as follows: the mean value of NAA was 2.45 ± 0.97 mmol/kg (normal control group value: 2.5 ± 0.6 mmol/kg), and the mean value of Cho was 3.73 ± 1.54 mmol/kg (normal control group value: 2.1 ± 0.4 mmol/kg). There was no statistically significant difference between the NAA-Cho levels of Group 1a cases and the normal control group values reported by Kreis et al. [10] ($P=0.921$ and $P=0.147$, respectively). The mean value of Cr was significantly lower than in the control group (2.48 ± 1.1 mmol/kg [control group: 4.5 ± 0.4 mmol/kg], $P<0.005$). The mean NAA/Cr ratio was 1.02 ± 0.14 mmol/kg

(control group: 0.56 ± 0.00 mmol/kg), and the mean Cho/Cr ratio was 1.54 ± 0.22 mmol/kg (control group: 0.47 ± 0.00 mmol/kg). These values were both significantly higher than in the control group ($P<0.05$). The mean NAA/Cho ratio was 0.66 ± 0.07 mmol/kg (control group: 1.19 ± 0.00 mmol/kg), and that value was statistically lower than in the control group ($P<0.05$). The MRS findings and comparisons with normal values are summarized in Tables 2 and 3.

The MRS findings of term newborns from Group 1b were as follows: the mean values of NAA and Cho were 3.26 ± 2.24 mmol/kg (control group: 3.4 ± 0.5 mmol/kg) and 3.63 ± 1.90 mmol/kg (control group: 2.2 ± 0.3 mmol/kg), respectively. Both mean NAA and Cho values showed no statistically significant difference when compared with control group values reported by Kreis et al. [10] ($P=0.892$ and $P=0.169$, respectively). The mean value of Cr was significantly lower than in the control group (2.69 ± 1.48 mmol/kg [control group: 4.8 ± 0.5 mmol/kg], $P<0.005$). The mean NAA/Cr ratio value was 1.19 ± 0.33 mmol/kg (control group: 0.71 ± 0.00 mmol/kg), and the mean Cho/Cr ratio value was 1.39 ± 0.26 mmol/kg (control group: 0.46 ± 0.00 mmol/kg). Both mean NAA/Cr and Cho/Cr values were significantly higher than in the control group ($P<0.05$). The mean NAA/Cho ratio was 0.87 ± 0.27 mmol/kg (control group: 1.55 ± 0.00 mmol/kg), and that value was statistically lower than in the control group ($P<0.05$) (Tables 4 and 5; Figure 2).

The mean NAA, Cho, and Cr values, and mean NAA/Cho, NAA/Cr, and Cho/Cr ratio values were compared between

Table 4. Group 1b (Term infants) MRS values.

Patient/sex/age(day)	TE (msec)	NAA (mmol/kg)	Cho (mmol/kg)	Cr (mmol/kg)	NAA/Cr	NAA/Cho	Cho/Cr
1/M/17	135	2.08	2.71	1.5	1.38	0.76	1.80
2/M/10	135	1.12	1.41	1.03	1.08	0.79	1.36
3/F/18	135	4.28	6.15	4.34	0.93	0.69	1.41
4/M/18	135	2.12	2.89	2.54	0.83	0.73	1.31
5/F/29	135	6.68	4.98	4.06	1.64	1.34	1.21

Normal values for term infants (Mean ± standard deviation); NAA – 3.4±0.5 mmol/kg; Cho – 2.2±0.3 mmol/kg; Cr – 4.8±0.5 mmol/kg; NAA/Cho – 1.55; NAA/Cr – 0.71; Cho/Cr – 0.46) [11].

Table 5. Group 1b (term infants) MRS values compared with the healthy control group.

Metabolites	Group 1b				Control group		
	Mean	St. deviation	Min.	Max.	Mean	St. deviation	P
NAA	3.26	2.24	1.12	6.68	3.40	0.50	0.892
Cho	3.63	1.90	1.41	6.15	2.20	0.30	0.169
Cr	2.69	1.48	1.03	4.34	4.80	0.50	0.034
NAA/Cho	0.87	0.27	0.70	1.34	1.55	0.00	0.005
NAA/Cr	1.19	0.33	0.83	1.65	0.71	0.00	0.030
Cho/Cr	1.39	0.26	1.14	1.81	0.46	0.00	0.001

Min. – minimum; Max. – maximum; St. deviation – standard deviation.

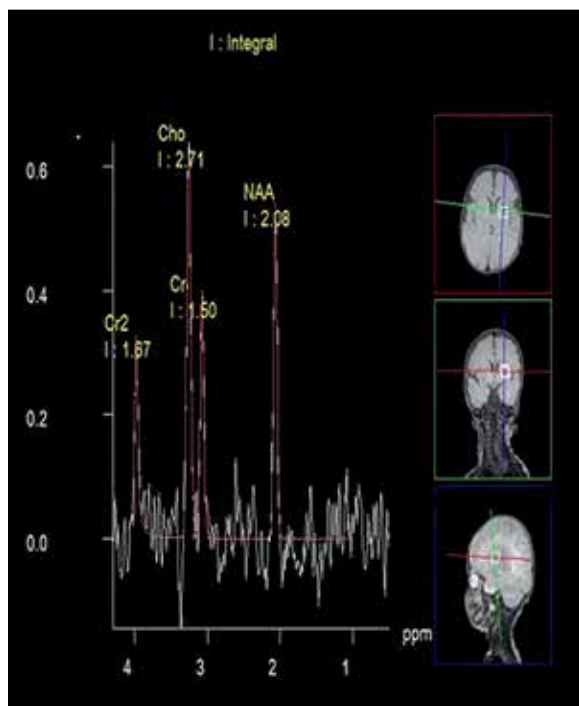


Figure 2. A 17-day-old male, single voxel MR spectroscopic examination demonstrated a decrease in Cr and NAA/Cho ratios, and an increase in NAA/Cr and Cho/Cr ratios.

Group 1a and 1b (preterm–term) cases, and no statistical difference was determined (P=0.730, P=0.905, P=0.905, and P=0.063, P=0.556, P=0.413, respectively) (Table 6).

Group 2 comprised 39 patients with chronic kernicterus. Depending on the accessible archive data, the mean birth weight of 20 patients was 3840±483.8 g (1825–3840 g), and the mean gestational weeks of 26 patients were 38.9±2 weeks (32–40 weeks). Mean TSB at admission was 34.2±7.02 mg/dL (25–45 mg/dL). Rh mismatch was found in nine patients (23%). ABO mismatch was determined in nine patients (23%), and glucose-6-phosphate dehydrogenase deficiency was found in one patient (2.6%). The etiology of hyperbilirubinemia in the remaining 20 patients was unknown (idiopathic, 51.3%). The findings of the kernicterus-related neurological physical examination were: strabismus in one case (2.6%), seizure in one case (2.6%), cerebral palsy in 19 cases (48.7%), seizure in cerebral palsy in 15 cases (38.4%), seizures and strabismus in cerebral palsy in one case (2.6%), and hearing loss in cerebral palsy in one case (2.6%). These findings were present in 38 patients (97.4%), and one case was physically normal (Table 7).

The mean age of Group 2 patients was 16.77±22.2 months (1–108 months) at the initial MR examination. Nine patients (23%) had normal MRI findings. Abnormal cerebral MRI changes in the remaining 30 patients (76.9%) were: symmetrical increased signal intensities on T2WI in GP in 24 patients (61.5%, most common pathological MRI finding), Dandy-Walker malformation in one case (2.6%),

Table 6. Comparison of the MRS values of patients in group 1a and group 1b.

Metabolites	Group 1a				Group 1b				p
	Mean	St. deviation	Min.	Max.	Mean	St. deviation	Min.	Max.	
NAA	2.45	0.97	1.39	3.63	3.26	2.24	1.12	6.68	0.730
Cho	3.73	1.54	2.21	5.41	3.63	1.90	1.41	6.15	0.905
Cr	2.48	1.10	1.20	3.40	2.69	1.48	1.03	4.34	0.905
NAA/Cho	0.66	0.07	0.60	0.76	0.87	0.27	0.70	1.34	0.063
NAA/Cr	1.02	0.14	0.82	1.16	1.19	0.33	0.83	1.65	0.556
Cho/Cr	1.54	0.22	1.37	1.84	1.39	0.26	1.14	1.81	0.413

Min. – minimum; Max. – maximum; St. deviation – standard deviation.

Table 7. Clinical and radiological findings of cases from Group 2.

Sex (M/F)	29/10
Birth weight: (gram) (mean ±SD)	2923±483.8
Total serum bilirubin: (mg/dL) (mean ±SD)	34.2±7
Treatment	n (%)
Blood exchange and phototherapy	19 (48.7)
Blood exchange transfusion	10 (25.6)
Phototherapy	10 (25.6)
Etiology	n (%)
Idiopathic	20 (51.3)
Rh incompatibility	9 (23)
ABO incompatibility	9 (23)
Glucose-6-phosphate dehydrogenase deficiency	1 (2.56)
Age at physical examination: (years) (mean ±SD)	3.0±2.7
Age at MRI examination: (months) (mean ±SD)	16.7±22.2
Neurological symptoms	n (%)
Cerebral palsy	19 (48.7)
Cerebral palsy and epilepsy	15 (38.5)
Normal neurological examination	1 (2.56)
Cerebral palsy, epilepsy and strabismus	1 (2.56)
Strabismus	1 (2.56)
Epilepsy	1 (2.56)
Cerebral palsy and hearing loss	1 (2.56)

cerebral atrophy in one case (2.6%), bifrontal mild sulcal enlargement in one case (2.6%), mild thinning of the callosal splenium and white matter with patches of increased signal intensity on the left side in one case (due to hypomyelination, 2.6%), enlargement of the third and lateral ventricles and cerebral fissures in one case (2.6%), cavum septum pellucidum et vergae in one case (2.6%), pathologically

increased signal intensities along the bilateral corticospinal tracts due to delayed myelination in one case (2.6%), mildly increased signal intensities in the lentiform nuclei in one case (2.6%), diffuse thinning in the corpus callosum in one case (2.6%), and patches of increased signal intensity adjacent to the occipital horns of the lateral ventricle in one case (2.6%).

The MRS findings of Group 2 patients (24 of 39 cases) were as follows: the mean value of NAA was 3.98 ± 1.58 mmol/kg (control group: 2.5 ± 0.6 mmol/kg) and the mean value of Cho was 3.39 ± 1.27 mmol/kg (control group: 2.1 ± 0.4 mmol/kg). There was a significant difference between the NAA-Cho levels of Group 2 cases and the control group values reported by Kreis et al. [10] ($P=0.001$ and $P=0.001$, respectively). The mean value of Cr was lower than in the control group (3.06 ± 1.23 mmol/kg [control group: 4.5 ± 0.4 mmol/kg], $P<0.005$). The mean NAA/Cr ratio was 1.32 ± 0.23 mmol/kg (control group: 0.56 ± 0.00 mmol/kg), and the mean Cho/Cr ratio was 1.11 ± 0.35 mmol/kg (control group: 0.47 ± 0.00 mmol/kg). Those values were significantly higher than in the control group ($P<0.05$). The mean NAA/Cho ratio value was 1.21 ± 0.27 mmol/kg (control group: 1.19 ± 0.00 mmol/kg), and that value was similar to the control group value ($P=0.938$). The MRS findings and comparisons with normal values are summarized in Table 8.

Seven patients (77.7%) were treated with phototherapy after blood exchange transfusion, and two patients (22.3%) were treated with phototherapy only in Group 1. Among Group 2 patients, 19 cases (48.7%) were treated with blood exchange transfusion and phototherapy while 10 cases (25.6%) were treated with phototherapy only and 10 cases (25.6%) with blood exchange transfusion only.

Discussion

Due to several etiologies (blood type mismatches, sepsis, enterohepatic circulation upregulation, enzyme deficiencies, bilirubin conjugation failures), hyperbilirubinemia may cause neurological disorders in newborns [11–14]. This entity is entitled kernicterus and generally occurs in hyperbilirubinemia if there was no treatment or the treatment was delayed. Treatment modalities include blood exchange and/or phototherapy [13]. Hyperbilirubinemia-related encephalopathy is initially detected during neurological

Table 8. Group 2 MRS values compared with the healthy control group.

Metabolites	Group 2				Control group		
	Mean	St. deviation	Min.	Max.	Mean	St. deviation	p
NAA	3.98	1.58	1.40	5.80	2.50	0.60	0.001
Cho	3.39	1.27	1.00	5.00	2.10	0.40	0.001
Cr	3.06	1.23	1.10	4.90	4.50	0.40	0.001
NAA/Cho	1.21	0.27	0.60	1.80	1.19	0.00	0.938
NAA/Cr	1.32	0.23	0.75	0.73	0.56	0.00	0.001
Cho/Cr	1.11	0.35	0.00	1.84	0.47	0.00	0.001

Min. – minimum; Max. – maximum; St. deviation – standard deviation.

physical examination, with findings such as lethargy, lack of nursing, opisthotonos, and bawling. Early encephalopathy symptoms could be similar to sepsis, asphyxia, and hypoglycemia [15]. Early neurological complications indicate poor prognosis [16]. In our study, the acute findings in Group 1 patients were hypotonia, lack of nursing, and lethargy. The chronic neurological sequelae of Group 2 patients were cerebral palsy, seizure, strabismus, and hearing loss (Table 7).

TSB levels of over 25–30 mg/dL can cause kernicterus [17]. In our study, the mean TSB levels of Group 1 and Group 2 cases were 31.1 ± 4.9 mg/dL and 34.2 ± 7.02 mg/dL, respectively. Hyperbilirubinemia encephalopathy, called kernicterus, occurs when bilirubin levels exceed albumin-binding capacity or if there is blood–brain barrier immaturity or damage, especially in premature and low birth weight babies [18]. Bilirubin neurotoxicity primarily damages the globus pallidus, subthalamic nucleus, substantia nigra, hippocampus, hypothalamus, nucleus of the 8th cranial nerve, inferior olivary nucleus, dentate nucleus, and certain thalamic nuclei [19]. A characteristic lesion form is symmetrical with temporary globus pallidus involvement [20]. MRI examinations have revealed that posteromedial globus pallidus is a more sensitive site of involvement in kernicterus [21]. Changes in thalamic and subthalamic nucleus signal intensity have also been reported [22–24]. The reason for this selective involvement pattern is unknown. Although certain parts of the brain are involved, changes in MRI signal intensity are especially distinct within the globus pallidus [23]. T2WI hyperintensity in the globus pallidus is a characteristic finding of late-term kernicterus, and was detected in 24 cases of Group 2 patients (61.5%) in our study.

There are limited studies regarding cerebral MRG and MRS changes in acute kernicterus. Cerebral MRI findings of acute kernicterus were initially reported in an eight-day-old infant by Penn et al. [25]. In that study, high-intensity lesions in T1WI were detected in the GP, internal capsule, and thalamus. After eight days, follow-up MRI sequences revealed abnormal T1WI signal increases in the hippocampus. The most striking finding in T2WI was diminishing demarcation of the GP, internal capsule, and anterior thalamus. In our study, one patient in Group 1 showed FLAIR and T2WI signal increase in the hippocampus. Haris et al.

reported cerebral MRI findings of four acute kernicterus cases (ages 5–21 days): T1WI hyperintensity in GP was reported in one case, and that change was not visible after 3–24 months in a follow-up MRI (that was the first study that revealed the temporality of MRI changes in kernicterus) [26]. The report also stated that there was no correlation between abnormal signal changes in T1WI and the long-term prognosis of the disease, but we believe that more extensive studies are necessary to reach the final conclusion. In our study, signal increases within GP were demonstrated in T1WI during the acute phase of all Group 1 cases. Additionally, T2WI and FLAIR images revealed mild cerebral white matter changes due to prematurity in four cases.

Martich-Kriss et al. [16] reported one-year follow-up MRI findings of a neurologically defective kernicterus infant. Bilateral T2 hyperintensity in GP was detected in the initial MRI when the infant was 18 days old, and that finding was still present in the six-month and one-year follow-up exams. We reported the results of the 4–6-month follow-up of seven patients from Group 1. In four cases, T1WI, T2WI, and FLAIR MRI sequences were normal. Mild enlargement of the lateral ventricles and minimal diffuse callosal thinning was detected in one case. Mild T2WI hyperintensities within GPi (globus pallidus interna) and GPe (globus pallidus externa) were detected in one case. In FLAIR and T2WI sequences, patches of increased signal intensity in the white matter adjacent to the occipital and frontal horns of the lateral ventricles were detected in one case.

We recommend further studies to reveal the relationship between acute-phase abnormal T1WI findings and chronic-phase T2WI MRI changes of kernicterus and the prognostic significance of these findings. Contrary to well-known T2WI signal increases within GP in chronic kernicterus, acute kernicterus cases reveal common and characteristic T1WI hyperintensity of GP.

Wang et al. [27] searched MRI findings of 24 kernicterus cases (age 6–18 days; two preterm and 22 term infants), and showed that increased signal intensity on T2WI in the basal ganglia and thalamus is a rare finding in acute kernicterus. However, GP hyperintensity on T1WI in 19 cases and subthalamic nucleus hyperintensity on T1WI in 10 cases were reported. In our study, there was no T2WI signal intensity change in nine acute kernicterus cases.

T1WI hyperintensity within GP has also been reported in the literature in relation to asphyxia, hepatic disorders, neurofibromatosis, total parenteral nutrition, and metastatic melanoma [28–31], but clinical manifestations generally help clinicians to differentiate these states from kernicterus.

Glutamate, the most common excitatory neurotransmitter of the brain, is excreted to the synaptic gaps by presynaptic neurons while excitatory synapse activation is converted to glycine by astrocytes after uptake [32]. Bilirubin inhibits glutamate uptake by astrocytes. Disruption of glutamate uptake and the glutamate–glycine cycle results in an increased Glu/Cr ratio in the synaptic gaps. Increased extracellular glutamate concentrations cause hyperexcitation of the postsynaptic neurotransmitter receptors (including N-methyl-D-aspartate, or NMDA), which can cause excitotoxic neuronal deaths [9]. Neuron culture-based *in-vitro* studies showed that bilirubin can be responsible for increased NMDA-receptor sensitivity. Taurine (2-aminoethanesulfonic acid) is classified as a single amino acid and plays an important role as a salt molecule in bile acid conjugation. Taurine is necessary for detoxification in the liver and essential for preventing excitotoxicity in the brain as an osmoregulator and neuromodulator [33]. Hyperexcitation of NMDA receptors induces taurine secretion and a high Tau/Cr ratio as a result of glutamate hypersecretion occurring in conclusion [34]. Intermediate-to-high levels of neuronal loss, demyelination, and gliosis are reported at the basal ganglia in the autopsies of kernicterus infants [35].

Wang et al. reported MRS findings of 24 kernicterus cases (age 6–18 days; two preterm and 22 term infants) and results of a statistical comparison with the control group.

References:

- Menkes JH: Textbook of Child Neurology, 5th ed, p613
- Cremer RJ, Perryman PW, Richards DH: Influence of light on the hyperbilirubinemia of infants. *Lancet*, 1958; 1: 1094–97
- Labrune P: Severe hyperbilirubinemia in the newborn: definition and management. *Arch Pediatr* 1998; 5: 1162–67
- Shapiro SM: Bilirubin toxicity in the developing nervous system. *Pediatr Neurol*, 2003; 29: 410–21
- Sugama S, Soeda A, Eto Y: Magnetic resonance imaging in three children with kernicterus. *Pediatr Neurol*, 2001; 25: 328–31
- Steinborn M, Seelos KC, Heuck A et al: MR findings in a patient with kernicterus. *Eur Radiol*, 1999; 9: 1939–45
- Govaert P, Lequin M, Swarte R et al: Changes in globus pallidus with (pre)term kernicterus. *Pediatrics*, 2003; 112: 1256–63
- Silva R, Mata L, Gulbenkian S et al: Inhibition of glutamate uptake by unconjugated bilirubin in cultured cortical rat astrocytes: role of concentration and pH. *Biochem Biophys Res Comm*, 1999; 265: 67–72
- McDonald J, Shapiro S, Silverstein F et al: Role of glutamate receptor-mediated excitotoxicity in bilirubin-induced brain injury in the Gunn rat model. *Exp Neurol*, 1998; 150: 21–29
- Kreis R, Hofmann L, Kuhlmann B et al: Brain metabolite composition during early human brain development as measured by quantitative *in vivo* H magnetic resonance spectroscopy. *Magn Reson Med*, 2002; 48: 949–58
- Brown A: I Erythrocyte metabolism and hemolysis in the newborn. *Pediatr Clin North Am*, 1966; 13: 879–903
- Newman AJ, Gross S: Hyperbilirubinemia in breast fed infants. *Pediatrics*, 1963; 32: 995–1001
- Devecioglu C, Katar S, Dogru O et al: Henna-induced hemolytic anemia and acute renal failure. *Turk J Pediatr*, 2001; 43: 65–66
- Arias IM, Wolfson S, Lucey JF: Transient familial neonatal hyperbilirubinemia. *J Clin Invest*, 1965; 44: 1442–50
- Friede RL: *Developmental Neuropathy*. Berlin: Springer-Verlag, 1989
- Martich-Kriss V, Kollias SS, Ball WS: MR findings in kernicterus. *Am J Neuroradiol*, 1995; 16: 819–21
- Piazza AJ, Stoll BJ, Kernicterus. In: Kliegman RM, Jenson HB, Berhman RE, Stanton BF (eds.). *Nelson Textbook of Pediatrics* (18th ed). Philadelphia: WB Saunders, 2007; 761–65
- Wennberg RP: The blood-brain barrier and bilirubin encephalopathy. *Cell Mol Neurobiol*, 2000; 20: 97–109
- Turkel SB, Miller CA, Guttenberg ME et al: A clinical pathologic reappraisal of kernicterus. *Pediatrics*, 1982; 69: 267–72
- Kim MH, Yoon JJ, Sher J et al: Lack of predictive indices in kernicterus: A comparison of clinical and pathologic factors in infant with or without kernicterus. *Pediatrics*, 1980; 66: 852–58
- Yokochi K: Magnetic resonance imaging in children with kernicterus. *Acta Paediatr*, 1995; 84: 937–39
- Sugama S, Soeda, Eto Y: Magnetic resonance imaging in three children with kernicterus. *Pediatr Neurol*, 2001; 25: 328–31
- Yilmaz Y, Ekinci G: Thalamic involvement in a patient with kernicterus. *Eur Radiol*, 2002; 12: 1837–39
- Steinborn M, Seelos KC, Heuck A et al: MR findings in a patient with kernicterus. *Eur Radiol*, 1999; 9: 1913–15
- Penn AA, Enzmann DR, Hahn JS et al: Kernicterus in a full term infant. *Pediatrics*, 1994; 93: 1003–6

Decreased NAA/Cho and NAA/Cr levels were revealed [27]. Similar to the study of Wang et al., Wu et al. (36) reported that the peak area ratios of NAA/Cr and NAA/Cho in the basal ganglia were significantly lower for their kernicterus group compared to the control group ($P < 0.05$). In the study, the NAA/Cr ratio reduction was related to neuronal axonal loss/disorder and an abnormal increase in gliosis. In our study, NAA/Cho levels were similarly decreased in Groups 1a and 1b ($P < 0.05$), but an elevated NAA/Cr ratio was established in all cases ($P < 0.05$).

In Group 2, increased NAA/Cr and Cho/Cr levels were evident ($P < 0.05$), but the NAA/Cho ratio was similar to the control group ($P = 0.938$). The NAA and Cho levels of Group 2 were increased, while the Cr levels were decreased in comparison to the control group ($P < 0.005$).

Cerebral MRS findings were investigated in six kernicterus infants (3–21 days old) by Oakden et al. [37]. Elevated Tau/Cr, Glx/Cr, and MI/Cr levels and decreased Cho/Cr levels were found ($P < 0.001$). No statistically significant difference was obtained for NAA/Cr levels ($P > 0.05$). In our study, the Cr levels of Group 1a and 1b were decreased compared to the control group ($P < 0.005$). However, contrary to the study of Oakden et al., in our study the Cho/Cr and NAA/Cr levels were increased ($P < 0.05$) in comparison to the control group reported by Kreis et al. [10].

Conclusions

MR imaging and 1H-MRS are important complementary tools in the diagnostics of neonatal bilirubin encephalopathy. This study provided important information for applying these MR modalities in the evaluation of neonates with bilirubin encephalopathy.

26. Harris MC, Bernbaum JC, Polin JR et al: Developmental follow-up of breastfed term and near-term infants with marked hyperbilirubinemia. *Pediatrics*, 2001; 107: 1075–80
27. Wang X, Wu W, Hou B et al: Studying neonatal bilirubin encephalopathy with conventional MRI, MRS, and DWI. *Neuroradiology*, 2008; 50: 885–93
28. Mirowitz SA, Sartor K, Gado M: High-intensity basal ganglia lesions on T1-weighted images in neurofibromatosis. *Am J Roentgenol*, 1990; 154: 369–73
29. Mirowitz SA, Westrich TJ, Hirsch JD: Hyperintense basal ganglia on T1-weighted MR images in patients receiving parenteral nutrition. *Radiology*, 1991; 181: 117–20
30. Gomori JM, Grossman RI, Shields JA et al: Choroidal melanomas: correlation of NMR spectroscopy and MR imaging. *Radiology*, 1986; 158: 443–45
31. Coskun A, Lequin M, Segal M et al: Quantitative analysis of MR images in asphyxiated neonates: correlation with neurodevelopmental outcome. *Am J Neuroradiol*, 2001; 22: 400–5
32. Silva R, Mata L, Gulbenkian S et al: Inhibition of glutamate uptake by unconjugated bilirubin in cultured cortical rat astrocytes: role of concentration and pH. *Biochem Biophys Res Comm*, 1999; 265: 67–72
33. Grojean S, Koziel V, Vert P et al: Bilirubin induces apoptosis via activation of NMDA receptors in developing rat brain neurons. *Exp Neurol*, 2000; 166: 334–41
34. Saransaari P, Oja SS: Taurine and neural cell damage. *Amino Acids*, 2000; 19: 509–26
35. Shapiro SM: Bilirubin toxicity in the developing nervous system. *Pediatr Neurol*, 2003; 29: 410–21
36. Wu W, Zhang P, Wang X et al: Usefulness of 1H-MRS in differentiating bilirubin encephalopathy from severe hyperbilirubinemia in neonates. *J Magn Reson Imaging*, 2013; 38(3): 634–40
37. Oakden WK, Moore AM, Blaser S et al: 1H-MR spectroscopic characteristics of kernicterus: a possible metabolic signature. *Am J Neuroradiol*, 2005; 26: 1571–74